Since January 2020 Elsevier has created a COVID-19 resource centre with free information in English and Mandarin on the novel coronavirus COVID-19. The COVID-19 resource centre is hosted on Elsevier Connect, the company's public news and information website.

Report

Current Biology

Cdk1 Phosphorylation of the Dam1 Complex Strengthens Kinetochore-Microtubule Attachments

Highlights

- Cdk1 phosphorylation of Dam1c strengthens kinetochore-microtubule attachments
- Ask1 is the key Cdk1 target in Dam1c that enhances for kinetochore-microtubule attachments
- Dynamic phosphorylation of Dam1c by Cdk1 is important *in vivo*
- Cdk1 phosphorylation of Ask1 appears to promote Dam1c oligomerization

Authors

Abraham Gutierrez, Jae ook Kim, Neil T. Umbreit, Charles L. Asbury, Trisha N. Davis, Matthew P. Miller, Sue Biggins

Correspondence

sbiggins@fredhutch.org

In Brief

Chromosome segregation requires attachments between kinetochores and microtubules. In budding yeast, the kinetochore complex Dam1 oligomerizes around microtubules to facilitate this connection. Gutierrez et al. show that the cell-cycle kinase Cdk1 phosphorylates the Dam1 complex to strengthen kinetochore-microtubule attachments during mitosis.

Gutierrez et al., 2020, Current Biology *30*, 4491–4499
November 16, 2020
https://doi.org/10.1016/j.cub.2020.08.054

CellPress

Current Biology

CellPress
OPEN ACCESS

Report

Cdk1 Phosphorylation of the Dam1 Complex Strengthens Kinetochore-Microtubule Attachments

Abraham Gutierrez,[1,2] Jae ook Kim,[3] Neil T. Umbreit,[3,5,6] Charles L. Asbury,[4] Trisha N. Davis,[3] Matthew P. Miller,[1,7] and Sue Biggins[1,8,*]

[1]Howard Hughes Medical Institute, Division of Basic Sciences, Fred Hutchinson Cancer Research Center, 1100 Fairview Avenue N, Seattle, WA 98109, USA
[2]Molecular and Cellular Biology Program, University of Washington, 1959 NE Pacific Street, Seattle, WA 98195, USA
[3]Department of Biochemistry, University of Washington, 1705 NE Pacific Street, Seattle, WA 98195, USA
[4]Department of Physiology and Biophysics, University of Washington, 1959 NE Pacific Street, Seattle, WA 98195, USA
[5]Present address: Howard Hughes Medical Institute, Department of Pediatric Oncology, Dana-Farber Cancer Institute, 450 Brookline Avenue, Boston, MA 02215, USA
[6]Present address: Department of Cell Biology, Harvard Medical School, 240 Longwood Avenue, Boston, MA 02115, USA
[7]Present address: Department of Biochemistry, University of Utah, 15 North Medical Drive East, Salt Lake City, UT 84112, USA
[8]Lead Contact
*Correspondence: sbiggins@fredhutch.org
https://doi.org/10.1016/j.cub.2020.08.054

SUMMARY

To ensure the faithful inheritance of DNA, a macromolecular protein complex called the kinetochore sustains the connection between chromosomes and force-generating dynamic microtubules during cell division. Defects in this process lead to aneuploidy, a common feature of cancer cells and the cause of many developmental diseases [1–4]. One of the major microtubule-binding activities in the kinetochore is mediated by the conserved Ndc80 complex (Ndc80c) [5–7]. In budding yeast, the retention of kinetochores on dynamic microtubule tips also depends on the essential heterodecameric Dam1 complex (Dam1c) [8–15], which binds to the Ndc80c and is proposed to be a functional ortholog of the metazoan Ska complex [16, 17]. The load-bearing activity of the Dam1c depends on its ability to oligomerize, and the purified complex spontaneously self-assembles into microtubule-encircling oligomeric rings, which are proposed to function as collars that allow kinetochores to processively track the plus-end tips of microtubules and harness the forces generated by disassembling microtubules [10–15, 18–22]. However, it is unknown whether there are specific regulatory events that promote Dam1c oligomerization to ensure accurate segregation. Here, we used a reconstitution system to discover that Cdk1, the major mitotic kinase that drives the cell cycle, phosphorylates the Ask1 component of the Dam1c to increase its residence time on microtubules and enhance kinetochore-microtubule attachment strength. We propose that Cdk1 activity promotes Dam1c oligomerization to ensure that kinetochore-microtubule attachments are stabilized as kinetochores come under tension in mitosis.

RESULTS AND DISCUSSION

Phosphorylation of the Native Dam1c Strengthens Kinetochore-Microtubule Attachments

To measure the contribution of the Dam1 complex (Dam1c) to the strength of tip-bound kinetochore-microtubule attachments, we used an *in vitro* reconstitution system. Wild-type kinetochore particles were purified from budding yeast cells by immunoprecipitating Dsn1, a conserved kinetochore protein (Figure S1) [23]. To obtain kinetochore particles lacking the Dam1c, we used *dad1-1* cells that contain a temperature-sensitive mutant in the Dam1c component Dad1 [24]. We confirmed that kinetochore particles purified from *dad1-1* cells (referred to as Dad1-1 kinetochores) grown at the non-permissive temperature lack the Dam1c, but otherwise retain the major core kinetochore components (Figure S1). To test the biophysical coupling strength of the Dad1-1 kinetochores to microtubule tips, we used an optical trap to exert tension on kinetochore-microtubule attachments. Kinetochore particles were linked to polystyrene microbeads that were captured in a laser trap and then placed at the plus ends of dynamic microtubules that were grown from microtubule seeds tethered to a slide (Figure 1A). Once a kinetochore-microtubule interaction was established, tensile force was applied and then gradually increased until the kinetochore ruptured from the microtubule tip [19, 23, 25]. To compare Dad1-1 versus wild-type kinetochores, we measured rupture forces for many individual kinetochore particles of each type (Figure 1B). For each population, the fraction of attachments that survived up to a given level of force was plotted and the mean rupture force was also calculated. Wild-type kinetochores ruptured over a range of forces, with a mean strength of 9.4 piconewtons (pN) (Figures 1B and 1D). Dad1-1 kinetochores were substantially weaker

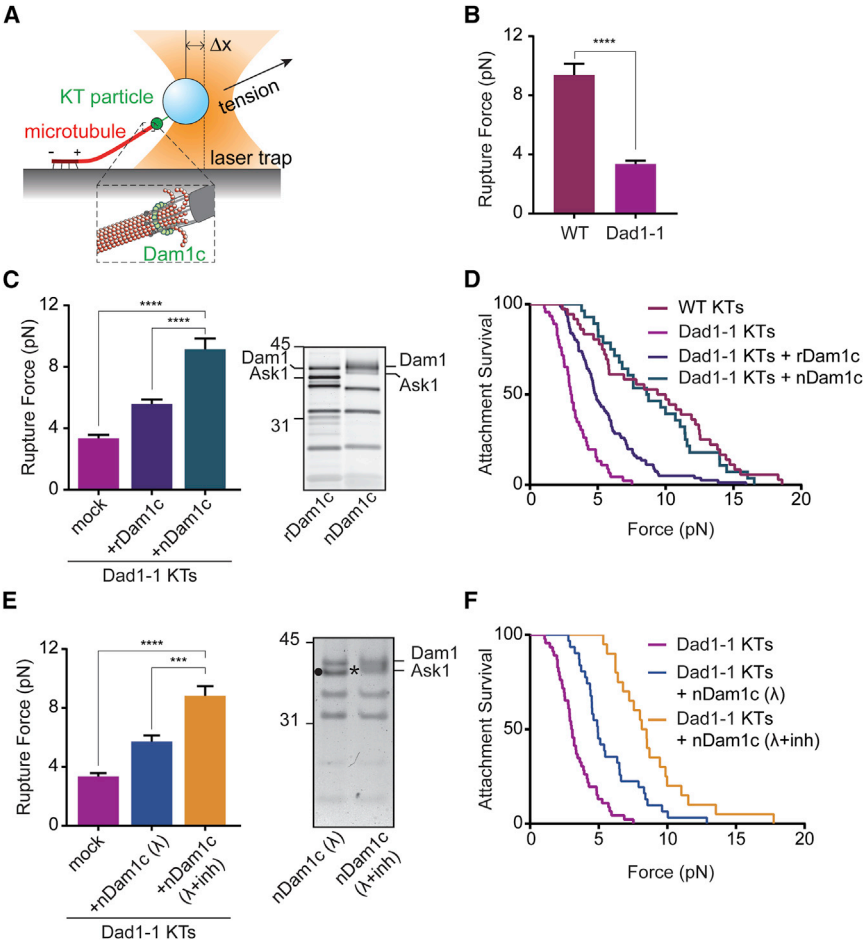

Figure 1. Phosphorylation of Native Dam1c Promotes Kinetochore-Microtubule Attachment Strength

(A) Schematic of the laser trap assay. Anchored microtubule seeds (dark red) are fixed to coverslips and dynamic microtubules (red) are grown from the plus ends. A bead (light blue sphere) linked to purified kinetochores (green dot) is attached to the tip of a microtubule using a laser trap and force is subsequently applied to the kinetochore-microtubule interface. The zoom-in (boxed) depicts an oligomerized Dam1c (green ring) around the microtubule that is connected to the rest of the kinetochore (gray).

(B) Mean rupture forces of wild-type (WT; SBY8253) and Dad1-1 (SBY8944) kinetochores (KTs). Error bars represent standard error of the mean (SEM; n = 36–46 events). p values were determined using a two-tailed unpaired t test (****p < 0.0001). See also Figure S1 and Tables S1 and S2.

(C) Mean rupture forces of Dad1-1 (SBY8944) KTs alone (mock), or with the addition of soluble recombinant Dam1 complex (rDam1c) or with native Dam1 complex (nDam1c; purified from SBY13538). The Dam1 complexes were analyzed by silver-stained SDS-PAGE (right). Molecular weight markers (kDa) are indicated and only the portion of the gel with the largest and most prominent Dam1c components is shown. Note that the entire bottom part of the gel is displayed, yet it is difficult to observe all ten of the Dam1c proteins by silver stain due to their small size. Error bars represent SEM (n = 28–81 events). p values were determined using a two-tailed unpaired t test (****p < 0.0001). See also Figure S1 and Tables S1 and S2.

(D) Attachment survival probability versus force for data in (B) and (C).

(E) Mean rupture forces of Dad1-1 kinetochores with the addition of soluble nDam1c (purified from SBY13538) that was treated with either phosphatase (λ) or phosphatase with inhibitors (λ + inh). Error bars represent SEM (n = 20–46 events). p values were determined using a two-tailed unpaired t test (***p < 0.0005, ****p < 0.0001). The Dam1 complexes that were added back were visualized by silver-stained SDS-PAGE. Dephosphorylated Ask1 migrates more quickly and is indicated by the black circle whereas phosphorylated Ask1 is indicated by the black asterisk. Molecular weight markers (kDa) are indicated on the left. See also Tables S1 and S2.

(F) Attachment survival probability versus force for data in (E) for Dad1-1 KTs alone or with an add-back of nDam1c that was treated with phosphatase or phosphatase with inhibitors.

(Figures 1B–1D). Their rupture force distribution was shifted to lower values and their mean strength was only 3.4 pN, consistent with previous measurements [19, 23]. To determine whether the reduced strength of the Dad1-1 kinetochores was solely due to the lack of the Dam1c, we purified recombinant Dam1c (rDam1c) from bacteria and performed add-back experiments [19]. When we introduced soluble rDam1c into the optical trapping assay with the kinetochore-bound beads, it rescued the strength of Dad1-1 kinetochores partially, increasing the average rupture force from 3.4 to 5.6 pN (Figures 1C and 1D), as observed previously [19]. One possible reason for the lack of a full rescue was that the recombinant complex lacked key post-translational modifications. To test this, we purified native Dam1c (nDam1c) from yeast cells and performed the same experiment. In contrast to rDam1c, the addition of nDam1c to Dad1-1 kinetochores fully restored kinetochore-microtubule attachment strength, increasing the mean rupture force to 9.1 pN (Figures 1C and 1D). This observation suggests that the native complex carries key modifications that contribute to its ability to hold microtubule tips under force and that are lacking on rDam1c.

Because the Dam1c is known to have multiple activities regulated by phosphorylation [10, 15, 25–36], we tested whether phosphorylation was responsible for the higher kinetochore-microtubule attachment strength observed with nDam1c relative to rDam1c. We treated purified nDam1c with phosphatase (λ) to remove phosphorylation or with phosphatase plus inhibitors (λ + inh) as a control. The migration of the Ask1 protein increased after phosphatase treatment (Figure 1E, silver-stained SDS-PAGE), indicating successful dephosphorylation. We then tested the activity of the dephosphorylated nDam1c in add-back assays as described above. As expected, the control-treated nDam1c fully rescued the Dad1-1 kinetochore particles, bringing their rupture strength up to 8.8 pN on average (Figures 1E and 1F). In contrast, the phosphatase-treated nDam1c only partially restored the mean rupture force to 5.7 pN, similar to rDam1c (Figures 1E and 1F). Taken together, these data indicate that Dam1c phosphorylation promotes stable kinetochore-microtubule attachments. Although this result was surprising given that Aurora B phosphorylation of the Dam1 component of the complex is known to weaken the interaction between

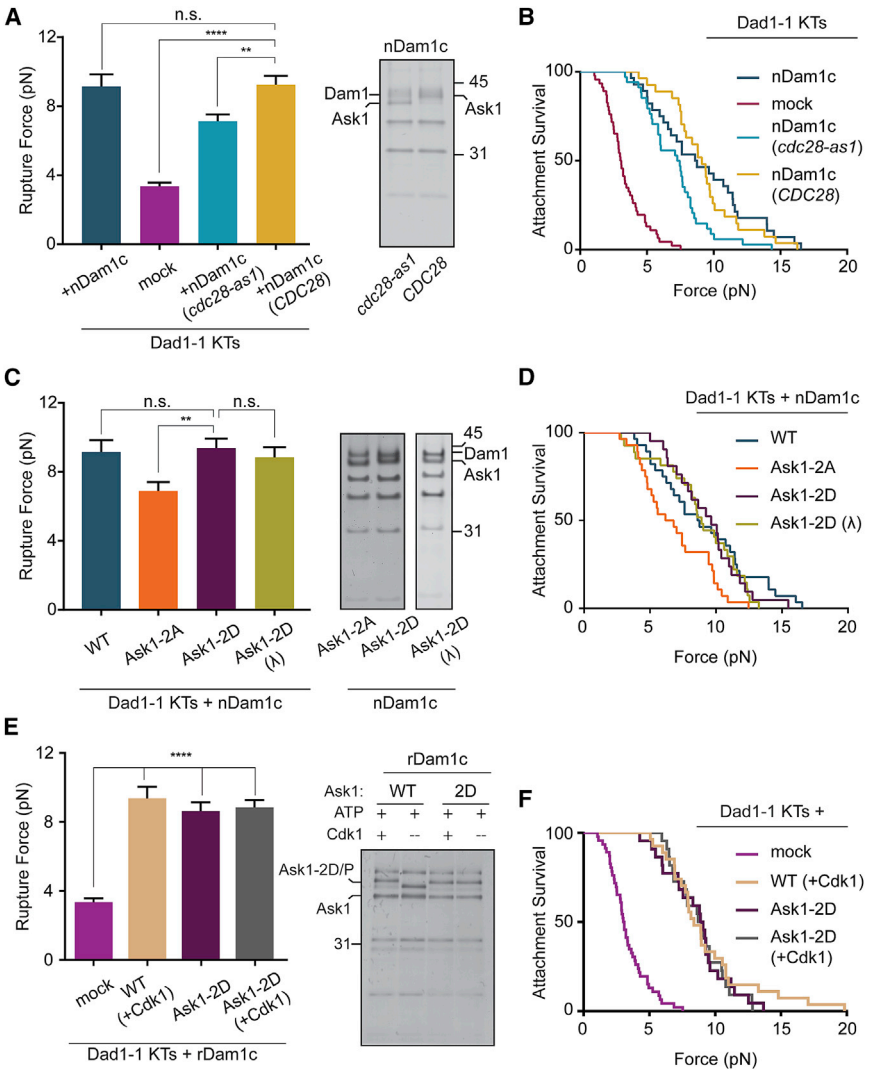

Figure 2. Cdk1-Mediated Phosphorylation of Ask1 Is Required for Wild-Type Kinetochore-Microtubule Attachment Strength

(A) Mean rupture forces for Dad1-1 KTs with the addition of soluble nDam1c that was purified from strains containing either analog-sensitive *cdc28-as1* (SBY13509) or wild-type *CDK1* (SBY12464) that had been treated with the analog 1-NM-PP-1 (left). Error bars represent SEM (n = 27–46 events). p values were determined using a two-tailed unpaired t test (n.s., not significant; $^{**}p < 0.005$, $^{****}p < 0.0001$). The mean rupture force data for Dad1-1 alone (mock) or with the addition of nDam1c come from Figure 1C. Purified Dam1c was visualized by silver-stained SDS-PAGE (right). Molecular weight markers (kDa) are indicated on the right. See also Figures S1–S3 and Tables S1 and S2.

(B) Attachment survival probability versus force for data in (A).

(C) Mean rupture forces for Dad1-1 KTs in the presence of soluble nDam1c that was purified from strains containing Ask1-S216A, S250A (Ask1-2A; SBY17833), or Ask1-S216D, S250D (Ask1-2D; SBY17833) that were untreated or phosphatase treated. Error bars represent SEM (n = 21–28 events). p values were determined using a two-tailed unpaired t test (n.s., not significant; $^{**}p < 0.005$). The mean rupture forces for Dad1-1 with nDam1c (WT) added back are from Figure 1C (left). The purified nDam1c was analyzed by silver-stained SDS-PAGE (right). See also Figure S2 and Tables S1 and S2.

(D) Attachment survival probability versus force for data in (C).

(E) Mean rupture forces for Dad1-1 KTs in the presence of soluble $rDam1c^{Ask1}$ or $rDam1c^{Ask1\text{-}2D}$ with or without Cdk1 phosphorylation. Error bars represent SEM (n = 22–27 events). p values were determined using a two-tailed unpaired t test ($^{****}p < 0.0001$). The mean rupture forces for Dad1-1 (mock) are from Figure 1C (left). The purified rDam1c was analyzed by silver-stained SDS-PAGE (right). See also Tables S1 and S2.

(F) Attachment survival probability versus force for data in (E).

kinetochores and microtubules [10, 15, 25–31, 33, 35, 36], our kinetochore and nDam1c purifications have little detectable phosphorylation on these sites [25].

Cdk1-Mediated Phosphorylation of Ask1 Enhances Kinetochore-Microtubule Attachment Strength

To further assess the role of Dam1c phosphorylation, we sought to identify the specific phosphorylation sites on nDam1c that contribute to kinetochore-microtubule attachment strength. The predominant migration shift of the purified Dam1c by silver-stained SDS-PAGE occurs on the Ask1 protein (Figure 1E, right). Ask1 phosphorylation increases as cells proceed into mitosis due to the major mitotic kinase Cdk1 (Cdc28 in *S. cerevisiae*), although the function of this phosphorylation is not known [34, 37, 38]. We therefore tested whether Cdk1 activity is required for nDam1c activity in the optical trap assay. To do this, we treated wild-type cells or those containing an analog-sensitive allele of Cdk1 (*cdc28-as1*) with the analog 1-NM-PP1 to specifically inhibit Cdk1 in the *cdc28-as1* cells [38, 39] prior to purifying nDam1c. Visualization of Ask1 on silver-stained SDS-PAGE showed that it migrated farther when purified from the analog-sensitive strain compared to wild type, indicating that the inhibitor worked and was specific to *cdc28-as1* cells (Figure 2A, right). We assayed the activity of the Dam1c purified from these two strains in add-back assays and found that the control nDam1c fully rescued Dad1-1 kinetochore particles, to an average rupture force of 9.2 pN, but nDam1c purified from *cdc28-as1* cells only partially rescued the mean rupture force to 7.1 pN (Figures 2A and 2B). We obtained similar results when nDam1c was purified from a temperature-sensitive mutant Cdk1 strain, *cdc28-13* [40] (Figure S2). Taken together, these data suggest that Cdk1 phosphorylation is required for the full contribution of the Dam1c to kinetochore-microtubule attachment strength. However, additional phosphorylation on the Dam1c may contribute to the interaction strength because the Dam1 complexes lacking Cdk1-mediated phosphorylation strengthened attachments more than rDam1c.

We suspected that Ask1 might be the relevant substrate because it was previously shown that Ask1 is phosphorylated by Cdk1 at the consensus sites S216 and S250 [34, 38]. To test the importance of the Cdk1 sites in Ask1, we mutated both residues to alanine (Ask1-2A) to block Cdk1-mediated phosphorylation. We then purified nDam1c from yeast cells expressing *ask1-2A* as the sole copy of the gene and tested this mutant complex (nDam1c$^{Ask1\text{-}2A}$) in our add-back optical trap assay. nDam1c$^{Ask1\text{-}2A}$ partially rescued the rupture force of Dad1-1 kinetochores to 6.9 pN (Figures 2C and 2D), which is similar to the strength measured with nDam1c purified from cells lacking Cdk1 activity. These results indicate that Cdk1 phosphorylation of one or both Ask1 sites is required for full Dam1c-dependent strengthening, and that additional Cdk1-independent phosphorylation of the Dam1c partially contributes to its function. Consistent with this idea, Ask1 phospho-mutants retained some Ask1 phosphorylation because phosphatase treatment increased their mobility by SDS-PAGE (Figure S3).

To further analyze the role of Cdk1 phosphorylation of Ask1, we tested whether nDam1c containing phospho-mimetic mutations in the Cdk1 target sites on Ask1 (nDam1c$^{Ask1\text{-}2D}$) could rescue the rupture force of the Dad1-1 kinetochores. The Dam1c was purified from *ask1-2D* cells and added back to the optical trap assay. nDam1c$^{Ask1\text{-}2D}$ fully rescued the rupture force to the wild-type level of 9.4 pN (Figures 2C and 2D). To test whether phosphorylation on the Cdk1 sites is sufficient for full Dam1c activity, we phosphatase treated nDam1c$^{Ask1\text{-}2D}$ prior to analysis in the optical trap assay. Remarkably, the phosphatase-treated nDam1c$^{Ask1\text{-}2D}$ was fully functional and rescued Dad1-1 kinetochores to 8.8 pN (Figures 2C and 2D). Therefore, although additional phosphorylation on nDam1c appears to contribute to its activity, Cdk1-mediated phosphorylation of Ask1 appears to be sufficient for the Dam1c to fully support kinetochore-microtubule attachments.

To further test whether Cdk1 phosphorylation of the Dam1c is sufficient to fully restore the strength of kinetochore-microtubule attachments to Dad1-1 kinetochores, we directly phosphorylated rDam1c with Cdk1. This led to a shift in the migration of Ask1, indicating the kinase reaction worked (Figure 2E, silver-stained SDS-PAGE). We added phosphorylated rDam1c to Dad1-1 kinetochores and performed the optical trap assay. Phosphorylated rDam1c fully rescued the rupture force to 9.3 pN (Figures 2E and 2F), suggesting that Cdk1 phosphorylation is sufficient to fully restore rDam1c activity. To test whether Cdk1 phosphorylation of Ask1 was the only relevant substrate, we assayed phospho-mimetic rDam1c (rDam1c$^{Ask1\text{-}2D}$) and found that it fully rescued the rupture force to 8.6 pN (Figures 2E and 2E). To verify there are no additional contributing Cdk1 phosphorylation sites on the Dam1c, we phosphorylated rDam1c$^{Ask1\text{-}2D}$ with Cdk1. There were no further migration shifts on the Ask1 protein after the Cdk1 kinase reaction when compared to Ask1-2D (Figure 2E, silver-stained SDS-PAGE). Consistent with this, the Cdk1-phosphorylated rDam1c$^{Ask1\text{-}2D}$ rupture force was 8.8 pN, which is similar to untreated rDam1c$^{Ask1\text{-}2D}$ (Figures 2E and 2F). Together, these data strongly suggest that even though other phosphorylation on the Dam1c might strengthen kinetochore-microtubule attachments, Cdk1 phosphorylation of the Ask1 protein is sufficient to fully restore the strength of kinetochore-microtubule attachments to Dad1-1 kinetochores.

Ask1 Phospho-regulation Is Important for Accurate Chromosome Segregation

We next asked whether Cdk1 phosphorylation of the Dam1c affects chromosome segregation *in vivo*. Although previous work found that the single- and double-phospho-mutants of Ask1 do not exhibit major growth defects, they were never analyzed for chromosome stability [34]. To assess chromosome segregation, we performed a quantitative chromosome transmission fidelity assay, or sectoring assay [41, 42]. This strategy utilizes a non-essential chromosome fragment III (CFIII) whose loss can be detected and quantified by a change in the color of the yeast cells. Both the *ask1-2A* and *ask1-2D* cells exhibited a significant increase in chromosome loss, with the *ask1-2A* cells exhibiting an eight-fold increase in chromosome missegregation compared to wild type (Figure 3A). Because both a lack of phosphorylation as well as a phospho-mimetic mutant of Ask1 lead to chromosome loss, it appears important that Dam1c phosphorylation is dynamically regulated *in vivo*. To further characterize the role of Ask1 phosphorylation, we asked whether defects in its regulation exhibit genetic interactions with mutations in other Dam1c components. We made double mutants containing the *dam1-9* allele that is mildly temperature sensitive in our strain background and assayed serial dilutions for growth at a semi-permissive temperature [43]. Whereas all of the single mutants were able to grow at 37°C, the *dam1-9 ask1-2A* cells were inviable (Figure 3B). To determine whether kinetochore function is affected in the double-mutant cells, we examined kinetochore biorientation in metaphase-arrested cells. The centromere of chromosome III was fluorescently marked by the binding of GFP-LacI to Lac operators [44]. When kinetochores biorient and come under tension, two centromere foci can be visualized. However, the practical resolution limit of the light microscope prevents us from visualizing separated foci unless they are at least 0.3 mm apart, so we were only able to resolve 28% of kinetochores as two bioriented foci in wild-type cells at 37°C. However, only 15% of *dam1-9* cells had two foci and this further decreased to 2% of the *dam1-9 ask1-2A* mutants (Figure 3C), suggesting these cells have a kinetochore biorientation defect. These data are consistent with phosphorylation of the Dam1c promoting kinetochore function *in vivo*.

Ask1 Phosphorylation Appears to Facilitate Dam1c Oligomerization

We next sought to address how Ask1 phosphorylation enhances Dam1c function to promote kinetochore-microtubule attachment strength. It was previously shown that Dam1c interacts with the kinetochore-microtubule-binding component Ndc80 to promote its association with microtubules, at both the lattice and at the plus-end tips [8, 10, 18]. In addition, Cdk1 phosphorylation of the vertebrate Ska complex directly promotes its interaction with Ndc80c [45, 46]. We therefore tested whether phosphorylation enhances the interaction between the Dam1c and the kinetochore-bound Ndc80c, but we found that the interaction was similar in the presence or absence of microtubules regardless of the phosphorylation state (Figure S4).

The Dam1c initially contacts microtubules as a monomer and then an estimated 17 individual complexes oligomerize into a ring around microtubules [47], so we next tested whether phosphorylation promotes either of these activities using

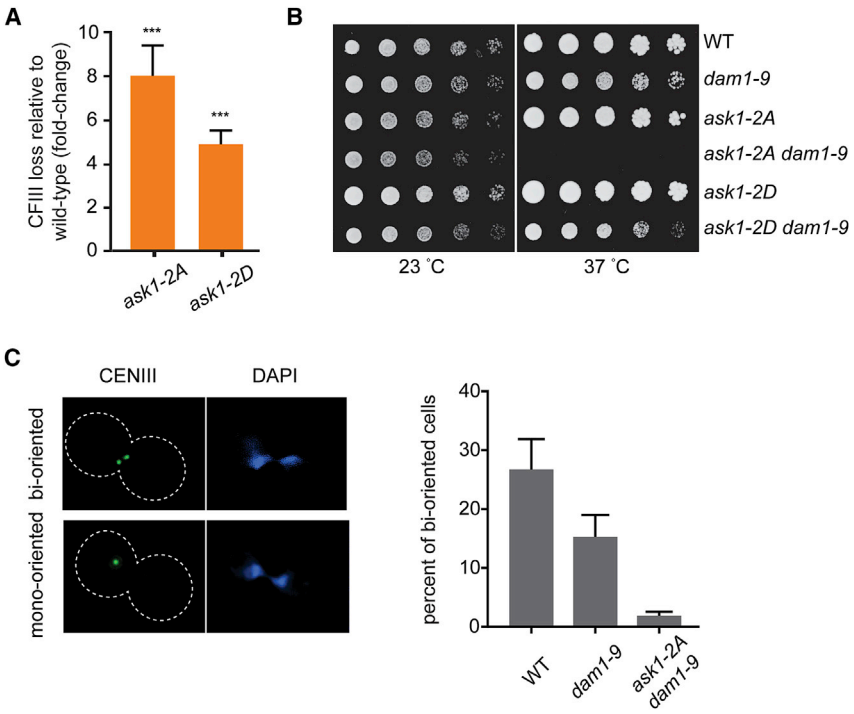

Figure 3. Dynamic Ask1 Phospho-regulation Is Important for Chromosome Stability *In Vivo*

(A) *Ask1-2A* (2A; SBY18724) and *ask1-2D* (2D; SBY18726) cells containing a non-essential chromosome fragment were analyzed for chromosome loss and the fold change relative to wild type was plotted. *Ask1-2A* and *ask1-2D* strains both had significant loss relative to wild type but not to each other. Error bars represent SEM (n = 5). Approximately 10,000 colonies were analyzed for each replicate for a total of five replicates. The statistical significance was determined using Student's t test (***p < 0.0005).

(B) Five-fold serial dilutions of wild-type (SBY18086), *dam1-9* (SBY19132), *ask1-2A* (SBY18088), *ask1-2A dam1-9* (SBY19136), *ask1-2D* (SBY18089), and *ask1-2D dam1-9* (SBY19138) cells were plated onto yeast media. Samples were grown at 23˚C (left) or 37˚C (right).

(C) Wild-type (SBY20049), *dam1-9* (SBY20050), and *dam1-9 ask1-2A* (SBY20052) cells containing fluorescently labeled chromosome III centromeres (CEN3) and methionine-repressible Cdc20 protein were grown at 37˚C for 2.5 h to arrest cells in metaphase. Microscopy was performed on metaphase-arrested cells as indicated by a single DNA mass (blue) to visualize the centromeres of chromosome III via LacI-GFP (green). Error bars represent SD of two independent experiments; at least 200 cells were counted for each experiment. Representative images are shown (left) and the percentage of bioriented cells was quantified (right).

single-molecule total internal reflection fluorescence (TIRF) microscopy [11, 18, 48–50]. First, we tested whether phosphorylation promotes the initial binding of Dam1c monomers to the lattice of the microtubule. To do this, we monitored the binding of single monomers on individual, Taxol-stabilized microtubules using a concentration of purified rDam1c (50 pM) that was low enough to prevent its oligomerization [15] (Figure 4A). We measured the residence times of the fluorescently labeled wild-type rDam1c$^{Ask1\text{-}GFP}$ and phospho-mimetic rDam1c$^{Ask1\text{-}2D\text{-}GFP}$ monomers on the microtubules and found that they behaved identically (Figures 4B and 4C), indicating that phosphorylation does not directly affect the interaction between microtubules and Dam1c monomers. Next, we tested whether Ask1 phosphorylation alters Dam1c oligomerization. To do this, we mixed a higher concentration of non-fluorescent "dark" rDam1c (1 nM), which promotes Dam1c oligomerization on the microtubules, together with a small amount of fluorescent "tracer" rDam1c (50 pM), to enable observation of individual monomers under these conditions (Figure 4D). It has previously been demonstrated that the residence times for individual, fluorescence-tagged, microtubule-binding subcomplexes are increased when they hetero-oligomerize with other, non-fluorescent microtubule binders [19, 29, 51]. We therefore mixed wild-type dark rDam1c^{Ask1} with the wild-type tracer rDam1c$^{Ask1\text{-}GFP}$ and found that the mean residence time of rDam1c$^{Ask1\text{-}GFP}$ was 8 s (Figures 4E and 4F), which is an ~2-fold increase over the residence time of rDam1c$^{Ask1\text{-}GFP}$ alone (Figures 4B and 4C). This increase in residence time is due to the formation of oligomers that bind more stably to the microtubules than monomers [19]. Strikingly, the residence time was more substantially increased, by 3-fold, when phospho-mimetic rDam1c$^{Ask1\text{-}2D}$ was used instead of wild-type rDam1c^{Ask1} (Figures 4E and 4F). This observation strongly suggests that phosphorylation of Ask1 promotes oligomerization of the Dam1c. Although the SARS-CoV-2 pandemic prevented us from attempting additional assays to analyze oligomerization, we note that previous studies demonstrated that increased residence time in the TIRF assay correlates with oligomerization when also assayed by electron microscopy [19, 29, 51].

To test whether the enhanced oligomerization of the Dam1c *in vitro* has a role *in vivo*, we analyzed cell growth in the presence of benomyl, a microtubule-destabilizing drug. Whereas wild-type and *ask1-2A* cells had difficulty growing on plates containing benomyl (Figure 4G), *ask1-2D* cells survived. These data suggest that microtubules are stabilized in *ask1-2D* cells, consistent with enhanced Dam1c oligomerization around the microtubule. We next tested whether Ask1 phosphorylation can suppress defects in oligomerization induced by Aurora B-dependent phosphorylation of another subunit of the Dam1c, the Dam1 protein. It was previously found that Aurora B-mediated phosphorylation of Dam1-S20 inhibits Dam1c oligomerization *in vitro* [29]. Consistent with this prior discovery, *dam1-S20D* cells were benomyl sensitive but the addition of the *ask1-2D* mutation suppressed the benomyl sensitivity (Figure 4G). This suppression indicates that the effect of *ask1-2D* opposes that of *dam1-S20D in vivo*, consistent with our finding that Ask1-2D appears to promote oligomerization *in vitro*, whereas phosphorylation of Dam1-S20 inhibits oligomerization. Taken together, these data strongly suggest that Cdk1 phosphorylation of Ask1 promotes oligomerization of the Dam1c in a cell-cycle-dependent manner to ensure accurate chromosome segregation.

The Dam1c promotes chromosome segregation through multiple functions that include directly binding to microtubules, interacting with the Ndc80 kinetochore complex, and oligomerizing

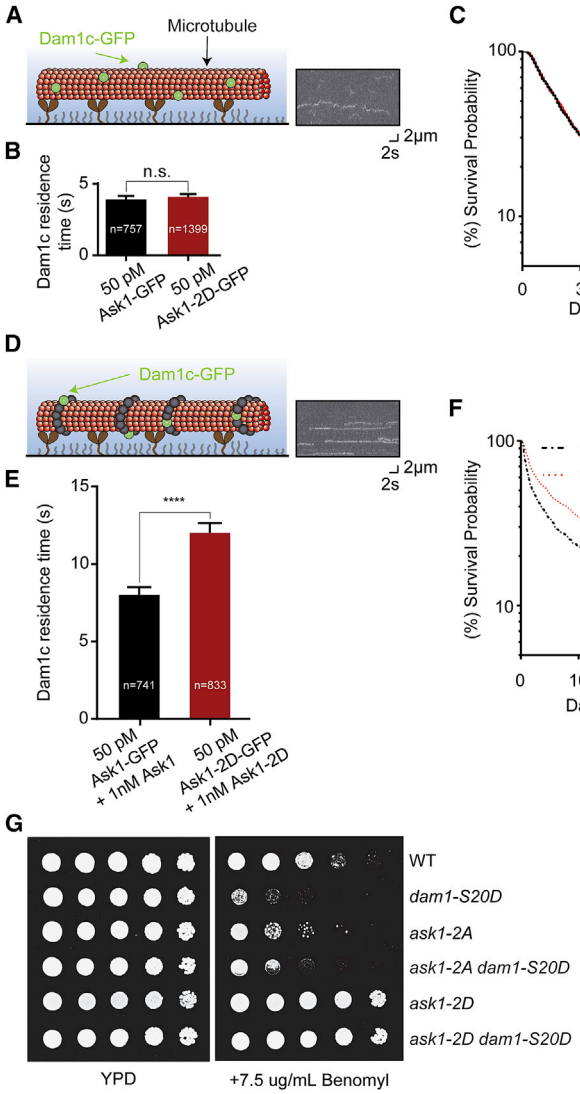

Figure 4. Ask1 Phosphorylation Promotes Dam1c Oligomerization

(A) Schematic of the TIRF assay used to analyze Dam1c monomer binding to microtubules. Dam1c binds to microtubules as a monomer at low concentrations (50 pM). To assay the effect of phosphorylation on these binding states, fluorescently labeled rDam1c (green spheres; Dad1-GFP) containing either rDam1c$^{Ask1\text{-}GFP}$ or rDam1c$^{Ask1\text{-}2D\text{-}GFP}$ at low monomeric concentration (50 pM) was added to microtubules and the residence time of Dam1c was recorded. A representative kymograph of rDam1c$^{Ask1\text{-}GFP}$ is shown (right). See also Figure S4.

(B) Average residence time of Dam1c on the microtubule with recombinant wild-type rDam1c$^{Ask1\text{-}GFP}$ or mutant rDam1c$^{Ask1\text{-}2D\text{-}GFP}$. Error bars represent average residence time ± error of the mean (n.s., not significant). See also Data S1.

(C) Attachment survival probability versus residence time for data in (B).

(D) Schematic of the TIRF assay used to monitor Dam1c oligomerization. To analyze oligomerization, a higher concentration of unlabeled dark rDam1c (1 nM; gray spheres) was added to fluorescently labeled monomeric Dam1c to promote oligomerization and the residence time of Dam1c was recorded. A representative rDam1c$^{Ask1\text{-}GFP}$ kymograph is shown.

(E) Average residence time of fluorescent recombinant wild-type 50 pM rDam1c$^{Ask1\text{-}GFP}$ or mutant 50 pM rDam1c$^{Ask1\text{-}2D\text{-}GFP}$ with an additional 1 nM dark rDam1c^{Ask1} or rDam1c$^{Ask1\text{-}2D}$, respectively. Error bars represent average residence time ± error of the mean (****$p < 0.0001$).

(F) Attachment survival probability versus residence time for data in (E). See also Data S1.

(G) Five-fold serial dilutions of wild-type (SBY19361), *dam1-S20D* (SBY18466), *ask1-2A* (SBY19314), *ask1-2A dam1-S20D* (SBY18468), *ask1-2D* (SBY19319), and *ask1-2D dam1-S20D* (SBY18469) cells were plated on media containing 2% glucose alone or with the addition of benomyl (7.5 μg/mL).

around the microtubule to ensure processive tracking of dynamic microtubule tips [15, 20–22, 36, 43, 48, 52–54]. Here, we identify a key phospho-regulatory mechanism that appears to promote Dam1c oligomerization to preserve the attachment of kinetochores to dynamic microtubules. Although it was previously known that Cdk1 phosphorylates the Ask1 component [34], the underlying function of the modifications was not known. Using biophysical techniques, we found that Cdk1 phosphorylation appears to promote the oligomerization of the Dam1c and does not affect the ability of the Dam1c to bind to microtubules, to the Ndc80c, or to kinetochores. Cdk1 phosphorylation of the Ska complex [45, 46] is also known to promote kinetochore function, consistent with it having functions analogous to the Dam1c [17, 55]. However, the underlying mechanism is different because the Ska complex does not appear to oligomerize around microtubules and Cdk1 phosphorylation enhances its direct interaction with the Ndc80c [45, 46]. Although a high-resolution structure of the Dam1c was recently solved using cryoelectron microscopy (cryo-EM) [47], the C-terminal portion of Ask1 that contains the Cdk1 phosphorylation sites was not present in the structure. However, crosslinking data suggest that the C-terminal region of Ask1 that contains the Cdk1 phosphorylation sites can interact with a second Dam1c monomer through Spc34 [29], bringing up the possibility that phosphorylation promotes this interaction. Future structural work will be required to elucidate the underlying contacts that are enhanced by phosphorylation to determine whether it alters intra- or inter-complex interactions.

Accurate chromosome segregation requires that every pair of sister kinetochores biorients and attaches to microtubules from opposite poles. However, early in mitosis, kinetochores initially make random attachments to microtubules, which results in some pairs of sister kinetochores that are attached to the same pole instead of opposite poles. These incorrect kinetochore-microtubule attachments must be destabilized, and previous work showed that phosphorylation of the Dam1c by the Aurora B protein kinase facilitates this process [10, 15, 25–30, 33, 56]. As mitosis proceeds and kinetochores make proper attachments to microtubules, the attachments must be stabilized to resist the tension that is generated by biorientation. While it has been

known that the kinetochore-bound Dam1c oligomerizes around microtubules to stabilize stable kinetochore-microtubule attachments, it has not been established whether Dam1c oligomerization is positively regulated. Our work suggests that Dam1 oligomerization is regulated through the cell cycle by Cdk1 phosphorylation, providing a mechanism to couple oligomerization to cell-cycle progression. We propose that Cdk1 phosphorylates the Dam1c later in mitosis, after Aurora B phosphorylation, to prevent premature stabilization of incorrect attachments. As mitosis proceeds, the global increase in Cdk1 activity will promote oligomerization as cells establish proper kinetochore-microtubule attachments and help maintain them as they come under tension. Oligomerization may also help kinetochores maintain processive attachments as cells subsequently undergo anaphase. However, there is less force on kinetochores during anaphase, so it is unclear whether phosphorylation on Ask1 is required for anaphase. Because Cdk1 phosphorylation is reversed by the Cdc14 phosphatase in budding yeast, it is likely that Cdc14 activity inhibits oligomerization. In this case, the phosphorylation sites may not be accessible to phosphatase activity until anaphase is complete. Because cells containing mutants that abolish Ask1 phosphorylation or mimic constitutive phosphorylation exhibit chromosome missegregation, the dynamics of oligomerization appear to be critical for accurate mitosis. In the future, it will be important to determine when Ask1 dephosphorylation occurs and what additional regulatory events control Dam1c oligomerization as well as what other vital kinetochore functions are mediated by Cdk1 kinase activity.

STAR★METHODS

Detailed methods are provided in the online version of this paper and include the following:

- KEY RESOURCES TABLE
- RESOURCE AVAILABILITY
  - Lead Contact
  - Materials Availability
  - Data and Code Availability
- EXPERIMENTAL MODEL AND SUBJECT DETAILS
- METHOD DETAILS
  - Strain construction: Yeast Strains and Plasmids
  - Construction of ASK1 mutant strains at the LEU2 locus
  - Protein biochemistry
  - Phosphatase treatment
  - Immunoblot and silver stain analysis
  - *In vitro* binding assays
  - Phosphorylation kinase assays
  - Spotting assay and chromosome loss assay
  - Analysis of kinetochore biorientation
  - Recombinant protein expression and purification
  - TIRF microscopy
  - Optical trap assays
- QUANTIFICATION AND STATISTICAL ANALYSIS

SUPPLEMENTAL INFORMATION

Supplemental Information can be found online at https://doi.org/10.1016/j.cub.2020.08.054.

ACKNOWLEDGMENTS

We are grateful to the Biggins, Davis, and Asbury labs for providing critical feedback on the manuscript. We also thank the Nasmyth, Shokat, and Barnes labs for providing yeast strains. A.G. was supported by a Ford Foundation predoctoral fellowship and M.P.M. was an HHMI Fellow of the Damon Runyon Cancer Research Foundation. This work was supported by NIH grants T32CA080416 (to M.P.M.), T32 GM008268 (to N.T.U.), R01GM040506 and R35GM130293 (to T.N.D.), R35GM134842 (to C.L.A.), and R01GM064386 (to S.B.). This work was also supported by the Genomics, Proteomics, and Scientific Imaging Shared Resources of the Fred Hutch/University of Washington Cancer Consortium (P30 CA015704). S.B. is an Investigator of the Howard Hughes Medical Institute.

AUTHOR CONTRIBUTIONS

Conceptualization, A.G., M.P.M., C.L.A., and S.B.; Methodology, A.G., J.o.K., M.P.M., T.N.D., C.L.A., and S.B.; Software, C.L.A.; Formal Analysis, A.G. and J.o.K.; Investigation, A.G., J.o.K., M.P.M., and N.T.U.; Writing – Original Draft, A.G. and S.B.; Writing – Review & Editing, J.o.K., M.P.M., C.L.A., and T.N.D.; Funding Acquisition, A.G., M.P.M., N.T.U., C.L.A., T.N.D., and S.B.; Resources, N.T.U.; Supervision, M.P.M., C.L.A., T.N.D., and S.B.

DECLARATION OF INTERESTS

The authors declare no competing interests.

Received: January 23, 2020
Revised: July 20, 2020
Accepted: August 14, 2020
Published: September 17, 2020

REFERENCES

1. Hassold, T., and Hunt, P. (2001). To err (meiotically) is human: the genesis of human aneuploidy. Nat. Rev. Genet. *2*, 280–291.
2. Cimini, D. (2008). Merotelic kinetochore orientation, aneuploidy, and cancer. Biochim. Biophys. Acta *1786*, 32–40.
3. Ben-David, U., and Amon, A. (2020). Context is everything: aneuploidy in cancer. Nat. Rev. Genet. *21*, 44–62.
4. Webster, A., and Schuh, M. (2017). Mechanisms of aneuploidy in human eggs. Trends Cell Biol. *27*, 55–68.
5. Wigge, P.A., and Kilmartin, J.V. (2001). The Ndc80p complex from *Saccharomyces cerevisiae* contains conserved centromere components and has a function in chromosome segregation. J. Cell Biol. *152*, 349–360.
6. DeLuca, J.G., Gall, W.E., Ciferri, C., Cimini, D., Musacchio, A., and Salmon, E.D. (2006). Kinetochore microtubule dynamics and attachment stability are regulated by Hec1. Cell *127*, 969–982.
7. Cheeseman, I.M., Chappie, J.S., Wilson-Kubalek, E.M., and Desai, A. (2006). The conserved KMN network constitutes the core microtubule-binding site of the kinetochore. Cell *127*, 983–997.
8. Doodhi, H., Kasciukovic, T., Gierlinski, M., Li, S., Clayton, L., and Tanaka, T.U. (2019). Error correction is driven by direct competition between microtubules for interaction with a kinetochore. bioRxiv. https://doi.org/10.1101/455873.
9. Tanaka, K., Kitamura, E., Kitamura, Y., and Tanaka, T.U. (2007). Molecular mechanisms of microtubule-dependent kinetochore transport toward spindle poles. J. Cell Biol. *178*, 269–281.
10. Lampert, F., Hornung, P., and Westermann, S. (2010). The Dam1 complex confers microtubule plus end-tracking activity to the Ndc80 kinetochore complex. J. Cell Biol. *189*, 641–649.
11. Westermann, S., Avila-Sakar, A., Wang, H.-W., Niederstrasser, H., Wong, J., Drubin, D.G., Nogales, E., and Barnes, G. (2005). Formation of a dynamic kinetochore-microtubule interface through assembly of the Dam1 ring complex. Mol. Cell *17*, 277–290.

12. Asbury, C.L., Gestaut, D.R., Powers, A.F., Franck, A.D., and Davis, T.N. (2006). The Dam1 kinetochore complex harnesses microtubule dynamics to produce force and movement. Proc. Natl. Acad. Sci. USA *103*, 9873–9878.

13. Grishchuk, E.L., Spiridonov, I.S., Volkov, V.A., Efremov, A., Westermann, S., Drubin, D., Barnes, G., Ataullakhanov, F.I., and McIntosh, J.R. (2008). Different assemblies of the DAM1 complex follow shortening microtubules by distinct mechanisms. Proc. Natl. Acad. Sci. USA *105*, 6918–6923.

14. Westermann, S., Wang, H.-W., Avila-Sakar, A., Drubin, D.G., Nogales, E., and Barnes, G. (2006). The Dam1 kinetochore ring complex moves processively on depolymerizing microtubule ends. Nature *440*, 565–569.

15. Tien, J.F., Umbreit, N.T., Gestaut, D.R., Franck, A.D., Cooper, J., Wordeman, L., et al. (2010). Cooperation of the Dam1 and Ndc80 kinetochore complexes enhances microtubule coupling and is regulated by Aurora B. J. Cell Biol. *189*, 713–723.

16. Welburn, J.P.I., Grishchuk, E.L., Backer, C.B., Wilson-Kubalek, E.M., Yates, J.R., III, and Cheeseman, I.M. (2009). The human kinetochore Ska1 complex facilitates microtubule depolymerization-coupled motility. Dev. Cell *16*, 374–385.

17. van Hooff, J.J.E., Snel, B., and Kops, G.J.P.L. (2017). Unique phylogenetic distributions of the Ska and Dam1 complexes support functional analogy and suggest multiple parallel displacements of Ska by Dam1. Genome Biol. Evol. *9*, 1295–1303.

18. Miranda, J.J., De Wulf, P., Sorger, P.K., and Harrison, S.C. (2005). The yeast DASH complex forms closed rings on microtubules. Nat. Struct. Mol. Biol. *12*, 138–143.

19. Umbreit, N.T., Miller, M.P., Tien, J.F., Ortolá, J.C., Gui, L., Lee, K.K., Biggins, S., Asbury, C.L., and Davis, T.N. (2014). Kinetochores require oligomerization of Dam1 complex to maintain microtubule attachments against tension and promote biorientation. Nat. Commun. *5*, 4951.

20. Lampert, F., Mieck, C., Alushin, G.M., Nogales, E., and Westermann, S. (2013). Molecular requirements for the formation of a kinetochore-microtubule interface by Dam1 and Ndc80 complexes. J. Cell Biol. *200*, 21–30.

21. Lacefield, S., Lau, D.T.C., and Murray, A.W. (2009). Recruiting a microtubule-binding complex to DNA directs chromosome segregation in budding yeast. Nat. Cell Biol. *11*, 1116–1120.

22. Kiermaier, E., Woehrer, S., Peng, Y., Mechtler, K., and Westermann, S. (2009). A Dam1-based artificial kinetochore is sufficient to promote chromosome segregation in budding yeast. Nat. Cell Biol. *11*, 1109–1115.

23. Akiyoshi, B., Sarangapani, K.K., Powers, A.F., Nelson, C.R., Reichow, S.L., Arellano-Santoyo, H., Gonen, T., Ranish, J.A., Asbury, C.L., and Biggins, S. (2010). Tension directly stabilizes reconstituted kinetochore-microtubule attachments. Nature *468*, 576–579.

24. Enquist-Newman, M., Cheeseman, I.M., Van Goor, D., Drubin, D.G., Meluh, P.B., and Barnes, G. (2001). Dad1p, third component of the Duo1p/Dam1p complex involved in kinetochore function and mitotic spindle integrity. Mol. Biol. Cell *12*, 2601–2613.

25. Sarangapani, K.K., Akiyoshi, B., Duggan, N.M., Biggins, S., and Asbury, C.L. (2013). Phosphoregulation promotes release of kinetochores from dynamic microtubules via multiple mechanisms. Proc. Natl. Acad. Sci. USA *110*, 7282–7287.

26. Keating, P., Rachidi, N., Tanaka, T.U., and Stark, M.J.R. (2009). Ipl1-dependent phosphorylation of Dam1 is reduced by tension applied on kinetochores. J. Cell Sci. *122*, 4375–4382.

27. Kang, J., Cheeseman, I.M., Kallstrom, G., Velmurugan, S., Barnes, G., and Chan, C.S.M. (2001). Functional cooperation of Dam1, Ipl1, and the inner centromere protein (INCENP)-related protein Sli15 during chromosome segregation. J. Cell Biol. *155*, 763–774.

28. Cheeseman, I.M., Anderson, S., Jwa, M., Green, E.M., Kang, J.s., Yates, J.R., III, Chan, C.S.M., Drubin, D.G., and Barnes, G. (2002). Phospho-regulation of kinetochore-microtubule attachments by the Aurora kinase Ipl1p. Cell *111*, 163–172.

29. Zelter, A., Bonomi, M., Kim, J.O., Umbreit, N.T., Hoopmann, M.R., Johnson, R., Riffle, M., Jaschob, D., MacCoss, M.J., Moritz, R.L., and Davis, T.N. (2015). The molecular architecture of the Dam1 kinetochore complex is defined by cross-linking based structural modelling. Nat. Commun. *6*, 8673.

30. Kalantzaki, M., Kitamura, E., Zhang, T., Mino, A., Novák, B., and Tanaka, T.U. (2015). Kinetochore-microtubule error correction is driven by differentially regulated interaction modes. Nat. Cell Biol. *17*, 421–433.

31. Shah, S.B., Parmiter, D., Constantine, C., Elizalde, P., Naldrett, M., Karpova, T.S., and Choy, J.S. (2019). Glucose signaling is connected to chromosome segregation through protein kinase A phosphorylation of the Dam1 kinetochore subunit in *Saccharomyces cerevisiae*. Genetics *211*, 531–547.

32. Shimogawa, M.M., Graczyk, B., Gardner, M.K., Francis, S.E., White, E.A., Ess, M., Molk, J.N., Ruse, C., Niessen, S., Yates, J.R., III., et al. (2006). Mps1 phosphorylation of Dam1 couples kinetochores to microtubule plus ends at metaphase. Curr. Biol. *16*, 1489–1501.

33. Gestaut, D.R., Graczyk, B., Cooper, J., Widlund, P.O., Zelter, A., Wordeman, L., Asbury, C.L., and Davis, T.N. (2008). Phosphoregulation and depolymerization-driven movement of the Dam1 complex do not require ring formation. Nat. Cell Biol. *10*, 407–414.

34. Li, Y., and Elledge, S.J. (2003). The DASH complex component Ask1 is a cell cycle-regulated Cdk substrate in *Saccharomyces cerevisiae*. Cell Cycle *2*, 143–148.

35. Pinsky, B.A., Kotwaliwale, C.V., Tatsutani, S.Y., Breed, C.A., and Biggins, S. (2006). Glc7/protein phosphatase 1 regulatory subunits can oppose the Ipl1/aurora protein kinase by redistributing Glc7. Mol. Cell. Biol. *26*, 2648–2660.

36. Li, Y., Bachant, J., Alcasabas, A.A., Wang, Y., Qin, J., and Elledge, S.J. (2002). The mitotic spindle is required for loading of the DASH complex onto the kinetochore. Genes Dev. *16*, 183–197.

37. Cheeseman, I.M., Brew, C., Wolyniak, M., Desai, A., Anderson, S., Muster, N., Yates, J.R., Huffaker, T.C., Drubin, D.G., and Barnes, G. (2001). Implication of a novel multiprotein Dam1p complex in outer kinetochore function. J. Cell Biol. *155*, 1137–1145.

38. Ubersax, J.A., Woodbury, E.L., Quang, P.N., Paraz, M., Blethrow, J.D., Shah, K., Shokat, K.M., and Morgan, D.O. (2003). Targets of the cyclin-dependent kinase Cdk1. Nature *425*, 859–864.

39. Bishop, A.C., Ubersax, J.A., Petsch, D.T., Matheos, D.P., Gray, N.S., Blethrow, J., Shimizu, E., Tsien, J.Z., Schultz, P.G., Rose, M.D., et al. (2000). A chemical switch for inhibitor-sensitive alleles of any protein kinase. Nature *407*, 395–401.

40. Lörincz, A.T., and Reed, S.I. (1986). Sequence analysis of temperature-sensitive mutations in the *Saccharomyces cerevisiae* gene *CDC28*. Mol. Cell. Biol. *6*, 4099–4103.

41. Duffy, S., and Hieter, P. (2018). The chromosome transmission fidelity assay for measuring chromosome loss in yeast. In Genome Instability: Methods and Protocols, M.M. Falconi, and G.W. Brown, eds. (Humana Press), pp. 11–19.

42. Hieter, P., Mann, C., Snyder, M., and Davis, R.W. (1985). Mitotic stability of yeast chromosomes: a colony color assay that measures nondisjunction and chromosome loss. Cell *40*, 381–392.

43. Cheeseman, I.M., Enquist-Newman, M., Müller-Reichert, T., Drubin, D.G., and Barnes, G. (2001). Mitotic spindle integrity and kinetochore function linked by the Duo1p/Dam1p complex. J. Cell Biol. *152*, 197–212.

44. Straight, A.F., Belmont, A.S., Robinett, C.C., and Murray, A.W. (1996). GFP tagging of budding yeast chromosomes reveals that protein-protein interactions can mediate sister chromatid cohesion. Curr. Biol. *6*, 1599–1608.

45. Zhang, Q., Sivakumar, S., Chen, Y., Gao, H., Yang, L., Yuan, Z., Yu, H., and Liu, H. (2017). Ska3 phosphorylated by Cdk1 binds Ndc80 and recruits Ska to kinetochores to promote mitotic progression. Curr. Biol. *27*, 1477–1484.e4.

46. Huis in 't Veld, P.J., Volkov, V.A., Stender, I.D., Musacchio, A., and Dogterom, M. (2019). Molecular determinants of the Ska-Ndc80

interaction and their influence on microtubule tracking and force-coupling. eLife *8*, e49539.

47. Jenni, S., and Harrison, S.C. (2018). Structure of the DASH/Dam1 complex shows its role at the yeast kinetochore-microtubule interface. Science *360*, 552–558.
48. Grishchuk, E.L., Efremov, A.K., Volkov, V.A., Spiridonov, I.S., Gudimchuk, N., Westermann, S., Drubin, D., Barnes, G., McIntosh, J.R., and Ataullakhanov, F.I. (2008). The Dam1 ring binds microtubules strongly enough to be a processive as well as energy-efficient coupler for chromosome motion. Proc. Natl. Acad. Sci. USA *105*, 15423–15428.
49. Joglekar, A.P., Bouck, D.C., Molk, J.N., Bloom, K.S., and Salmon, E.D. (2006). Molecular architecture of a kinetochore-microtubule attachment site. Nat. Cell Biol. *8*, 581–585.
50. Ramey, V.H., Wang, H.-W., Nakajima, Y., Wong, A., Liu, J., Drubin, D., Barnes, G., and Nogales, E. (2011). The Dam1 ring binds to the E-hook of tubulin and diffuses along the microtubule. Mol. Biol. Cell *22*, 457–466.
51. Kim, J.O., Zelter, A., Umbreit, N.T., Bollozos, A., Riffle, M., Johnson, R., MacCoss, M.J., Asbury, C.L., and Davis, T.N. (2017). The Ndc80 complex bridges two Dam1 complex rings. eLife *6*, e21069.
52. Janke, C., Ortíz, J., Tanaka, T.U., Lechner, J., and Schiebel, E. (2002). Four new subunits of the Dam1-Duo1 complex reveal novel functions in sister kinetochore biorientation. EMBO J. *21*, 181–193.
53. Hofmann, C., Cheeseman, I.M., Goode, B.L., McDonald, K.L., Barnes, G., and Drubin, D.G. (1998). *Saccharomyces cerevisiae* Duo1p and Dam1p, novel proteins involved in mitotic spindle function. J. Cell Biol. *143*, 1029–1040.
54. Jin, F., and Wang, Y. (2013). The signaling network that silences the spindle assembly checkpoint upon the establishment of chromosome bipolar attachment. Proc. Natl. Acad. Sci. USA *110*, 21036–21041.
55. Zhang, Q., Chen, Y., Yang, L., and Liu, H. (2018). Multitasking Ska in chromosome segregation: its distinct pools might specify various functions. BioEssays *40*, 1700176.
56. Lampson, M.A., and Grishchuk, E.L. (2017). Mechanisms to avoid and correct erroneous kinetochore-microtubule attachments. Biology (Basel) *6*, 1.
57. Franck, A.D., Powers, A.F., Gestaut, D.R., Gonen, T., Davis, T.N., and Asbury, C.L. (2007). Tension applied through the Dam1 complex promotes microtubule elongation providing a direct mechanism for length control in mitosis. Nat. Cell Biol. *9*, 832–837.
58. Akiyoshi, B., and Biggins, S. (2010). Cdc14-dependent dephosphorylation of a kinetochore protein prior to anaphase in *Saccharomyces cerevisiae*. Genetics *186*, 1487–1491.
59. Spencer, F., Gerring, S.L., Connelly, C., and Hieter, P. (1990). Mitotic chromosome transmission fidelity mutants in *Saccharomyces cerevisiae*. Genetics *124*, 237–249.
60. Schindelin, J., Arganda-Carreras, I., Frise, E., Kaynig, V., Longair, M., Pietzsch, T., Preibisch, S., Rueden, C., Saalfeld, S., Schmid, B., et al. (2012). Fiji: an open-source platform for biological-image analysis. Nat. Methods *9*, 676–682.
61. Longtine, M.S., McKenzie, A., III, Demarini, D.J., Shah, N.G., Wach, A., Brachat, A., Philippsen, P., and Pringle, J.R. (1998). Additional modules for versatile and economical PCR-based gene deletion and modification in *Saccharomyces cerevisiae*. Yeast *14*, 953–961.
62. Miller, M.P., Evans, R.K., Zelter, A., Geyer, E.A., MacCoss, M.J., Rice, L.M., Davis, T.N., Asbury, C.L., and Biggins, S. (2019). Kinetochore-associated Stu2 promotes chromosome biorientation in vivo. PLoS Genet. *15*, e1008423.
63. Powers, A.F., Franck, A.D., Gestaut, D.R., Cooper, J., Gracyzk, B., Wei, R.R., Wordeman, L., Davis, T.N., and Asbury, C.L. (2009). The Ndc80 kinetochore complex forms load-bearing attachments to dynamic microtubule tips via biased diffusion. Cell *136*, 865–875.
64. Wei, R.R., Sorger, P.K., and Harrison, S.C. (2005). Molecular organization of the Ndc80 complex, an essential kinetochore component. Proc. Natl. Acad. Sci. USA *102*, 5363–5367.
65. Gestaut, D.R., Cooper, J., Asbury, C.L., Davis, T.N., and Wordeman, L. (2010). Reconstitution and functional analysis of kinetochore subcomplexes. Methods Cell Biol. *95*, 641–656.

STAR★METHODS

KEY RESOURCES TABLE

REAGENT or RESOURCE	SOURCE	IDENTIFIER
Antibodies		
Flag M2	Sigma-Aldrich	Cat# F3165; RRID: AB_259529
V5 E10/V4RR	Thermo Fisher Scientific	Cat# MA5-15253; RRID: AB_10977225
GFP JL-8	Living Colors	Cat# 632380; RRID: AB_10013427
Myc 9E10	Thermo Fisher Scientific	Cat# 13-2500; RRID: AB_2533008
(Polyclonal) Dam1 complex	Pacific Immunology	N/A
Chemicals, Peptides, and Recombinant Proteins		
1-NM-PP1	Toronto Research Chemical	Cat# A603003
Lambda Protein Phosphatase	New England Biolabs	Cat# P0753L
SNAP-Surface 647 dye	New England Biolabs	Cat# S9136S
CLIP-Surface 547 dye	New England Biolabs	Cat# S9233S
Recombinant Dam1 and Ndc80 complex	[15, 18, 51, 57]	N/A
Experimental Models: Organisms/Strains		
S. cerevisiae; Strain background: W303	This study	N/A
SBY3 (W303); *MATa ura3-1 leu2-3,112 his3-11 trp1-1 can1-100 ade2-1 bar1-1*	This study	N/A
SBY8253; SBY3, *DSN1-6His-3Flag:URA3*	This study	N/A
SBY8944; SBY3, *DSN1-6His-3Flag dad1-1:KanMx*	This study	N/A
SBY12464; SBY3, *DAD1-3Flag:TRP1*	This study	N/A
SBY13507; SBY3, *DAD1-3Flag:TRP1 cdc28-13*	This study [58]	N/A
SBY13509; SBY3, *DAD1-3Flag:TRP1 cdc28-as1*	This study [58]	N/A
SBY13538; SBY3, *DAD1-3V5:HIS*	This study	N/A
SBY16766; SBY3, *DAD1-SNAP-3V5:KanMx*	This study	N/A
SBY16826; SBY3, *MTW1-CLIP:KanMx dad1-1:KanMx*	This study	N/A
SBY16828; SBY3, *DSN1-His-Flag:URA3 MTW1-CLIP:KanMx dad1-1:KanMx*	This study	N/A
SBY17831; SBY3, *DAD1-3Flag:TRP1 ask1::KanMx leu2-3,112::ask1-S216A, S250A:LEU2*	This study	N/A
SBY17833; SBY3, *DAD1-3Flag:TRP1 ask1::KanMx leu2-3,112::ask1-S216D, S250D:LEU2*	This study	N/A
SBY18086; SBY3, *ask1::KanMx leu2-3,112::ASK1:LEU2*	This study	N/A
SBY18088; SBY3, *ask1::KanMx leu2-3,112::ask1-S216A, S250A:LEU2*	This study	N/A
SBY18466; SBY3, *DSN1-6His-3Flag:URA3 dam1(S20D):KanMx ask1::KanMx leu2-3,112::ASK1:LEU2*	This study [25, 28]	N/A
SBY18468; SBY3, *DSN1-6His-3Flag:URA3 dam1(S20D):KanNMx ask1::KanMx leu2-3,112::ask1-S216A, S250A:LEU2*	This study	N/A
SBY18469; SBY3, *DSN1-6His-3Flag:URA3 dam1(S20D):KanMx ask1::KanMx leu2-3,112::ask1-S216D, S250D:LEU2*	This study	N/A
SBY18606; SBY3, *CDC28-3V5:KanMx*	This study	N/A
SBY18722; SBY3, CFIII (CEN3.L.YPH278)*URA3-SUP11 ask1::KanMx leu2-3,112::ASK1:LEU2*	This study [59]	N/A

(*Continued on next page*)

Continued

REAGENT or RESOURCE	SOURCE	IDENTIFIER
SBY18724; SBY3, CFIII (CEN3.L.YPH278)*URA3-SUP11 ask1::KanMx leu2-3,112::ask1-S216A, S250A:LEU2*	This study [59]	N/A
SBY18726; SBY3, CFIII (CEN3.L.YPH278)*URA3-SUP11 ask1::KanMx leu2-3,112::ask1-S216D, S250D:LEU2*	This study [59]	N/A
SBY19132; SBY3, *dam1-9:kanMx ask1::KanMx leu2-3,112::ASK1:LEU2*	This study	N/A
SBY19136; SBY3, *dam1-9:kanMx ask1::KanMx leu2-3,112::ask1-S216A, S250A:LEU2*	This study	N/A
SBY19138; SBY3; *dam1-9::kanMX ask1::KanMx6 leu2-3,112::Ask1-S216D, S250D:LEU2*	This study	N/A
SBY19314; SBY3, *DSN1-6His-3Flag: URA3 ask1::KanMx leu2-3,112::ask1-S216A, S250A:LEU2*	This study	N/A
SBY19319; SBY3, *DSN1-6His-3Flag: URA3 ask1::KanMx leu2-3,112::ask1-S216D, S250D:LEU2*	This study	N/A
SBY19361; SBY3, *DSN1-6His-3Flag:URA3 ask1::KanMx leu2-3,112::ASK1:LEU2*	This study	N/A
SBY20049; SBY3, *pMET-CDC20:TRP1 cenIII-lacO128:TRP1 ask1::KanMx6 leu2-3,112::ASK1:LEU2 his3-11:pCUP1-GFP12-LacI12*	This study	N/A
SBY20050; SBY3, *pMET-CDC20:TRP1 cenIII-lacO128:TRP1 ask1::KanMx6 leu2-3,112::ASK1:LEU2 his3-11:pCUP1-GFP12-LacI12 dam1-9*	This study	N/A
SBY20052; SBY3, *pMET-CDC20:TRP1 cenIII-lacO128:TRP1 ask1::KanMx6 leu2-3,112::ASK1-S216A, S250A:LEU2 his3-11:pCUP1-GFP12-LacI12 dam1-9*	This study	N/A
Oligonucleotides		
See Table S3 for primer sequences	This study	N/A
Software and Algorithms		
Igor Pro	Wavemetrics	https://www.wavemetrics.com/; RRID: SCR_000325
LabVIEW	National Instruments	https://www.ni.com/; RRID: SCR_014325
ImageJ	NIH image	https://imagej.net/; RRID: SCR_003070
Fiji	[60]	http://fiji.sc; RRID: SCR_002285
PRISM	GraphPad Software	https://www.graphpad.com/scientific-software/prism/; RRID: SCR_002798
NIS-Elements Software	Nikon	https://www.microscope.healthcare.nikon.com/products/software/; RRID: SCR_014329

RESOURCE AVAILABILITY

Lead Contact

Further information and requests for resources and reagents should be directed to and will be fulfilled by the Lead Contact, Sue Biggins (sbiggins@fredhutch.org).

Materials Availability

Yeast strains generated by this study are available upon request.

Data and Code Availability

The published article includes all datasets generated or analyzed during this study.

EXPERIMENTAL MODEL AND SUBJECT DETAILS

Saccharomyces cerevisiae strains used in this study are derived from or backcrossed to be isogenic with W303. Yeast were cultured in standard yeast extract peptone dextrose (YPD) medium at 23°C unless indicated otherwise. Strains used in this study are listed in Key Resources Table.

METHOD DETAILS

Strain construction: Yeast Strains and Plasmids

Saccharomyces cerevisiae strains used in this study are derived from or backcrossed to SBY3 to be isogenic with the W303 background and are listed in Key Resources Table. All strains containing the following epitope-tagged genes are generated by standard PCR-based integration techniques at the endogenous loci as described in [61] and are fully functional. Primer sequences are listed in Table S3. *DSN1-6His-3Flag* is described in [23]. *DAD1-3V5* was made with primers SB4448 and SB4449 and template plasmid pSB2047. *DAD1-3Flag* was made with primers SB4214 and SB4215 and template plasmid pSB1265. *MTW1-CLIP* was made with primers SB3109 and SB3111 and template plasmid pSB1824. *DAD1-SNAP-3V5* as made with primers SB5091 and SB5092 and template plasmid pSB2402. *CDC28-3V5* was made with primers SB5892 and SB5893 and template plasmid pSB2068. The *dam1-S20D* mutant originates from David Drubin's lab (DDY2486) [28] and was backcrossed to SBY3. *Dam1-S20D* strains were derived from SBY3720 and were used in previous work [25]. *ASK1* plasmids were constructed as follows. *ASK1* was amplified by PCR using a primer containing sequence upstream of the *ASK1* gene and a recognition site for the restriction enzyme XhoI (SB5468) and a primer downstream of the *ASK1* stop codon with a recognition site for the restriction enzyme EagI (SB5469). The PCR product and a *LEU2* integrating vector (pSB2223) were digested with XhoI and Eag1 and ligated to create pSB2900. This plasmid was used as a template to make site directed mutations at *ASK1-S216* and *S250*, switching serine to alanine (pSB2904) by site directed mutagenesis with primers SB5602 and SB5604 or altering serine to aspartic acid (pSB2905) with primers SB5603 and SB5605. All plasmids were verified by sequencing. The non-essential yeast chromosome fragment strain was a gift of the Kim Nasmyth (YPH278) [59] and backcrossed to W303. *Cdc28-as1* was a gift from the Shokat lab and backcrossed into the W303 strain and used in [23].

Construction of ASK1 mutant strains at the LEU2 locus

The following steps created strains in which *ask1* mutants were integrated at the *LEU2* locus and the endogenous *ASK1* gene was deleted. First, a heterozygous *ASK1/ask1* diploid strain was generated (SBY17818) by deleting one copy of *ASK1* by PCR integration with PCR product produced with primers SB5523 and SB5524 and template plasmid pSB54 as described in [61]. The *ASK1* deletion was verified by PCR with primers SB5532 and SB5121 and then subsequently by tetrad dissection that resulted in 2:2 viability. The various *ASK1* plasmids (plasmids pSB2900, pSB2904, and pSB2905, described above) were digested with SwaI and transformed into SBY17818 to integrate them at the *LEU2* locus and then dissected to identify the correct genotypes.

Protein biochemistry

Native kinetochores and kinetochore subcomplexes were purified from either conditionally treated or asynchronously grown cells. Cells containing *cdc28-as1* were grown to OD_{600} 0.6-1.0 and then arrested in G1 with alpha factor (1 μg/mL in DMSO) for 3 hr, and at 2.5 hr the compound 1-NM-PP1 (0.5 μM in DMSO; Toronto Research Chemical, A603003) was added. Cells were washed twice to remove alpha-factor with equal volumes of YPD containing 0.5 μM of 1-NM-PP1. Cells were then resuspended in YPD with 5.0 μM of 1-NM-PP1 for 2-2.5 hr before cells were harvested. Cells from the *cdc28-13* temperature sensitive strain were shifted to the non-permissive temperature (37°C) for 2.5 hr before harvesting. Protein lysate was prepared by lysing cells with a magnetic impact bar submerged in liquid nitrogen using a Freezer/Mill (SPEX SamplePrep). Lysed cells were resuspended in buffer H (BH) (25 mM HEPES pH 8.0, 2 mM MgCl2, 0.1 mM EDTA, 0.5 mM EGTA, 0.1% NP-40, 15% glycerol with 150 mM KCl for native kinetochores) containing protease inhibitors (at 20 μg/mL final concentration for each of leupeptin, pepstatin A, chymostatin and 200 μM phenylmethylsulfonyl fluoride) and phosphatase inhibitors (0.1 mM Na-orthovanadate, 0.2 μM microcystin, 2 mM β-glycerophosphate, 1 mM Na pyrophosphate, 5 mM NaF) followed by ultracentrifugation at 24,000 RPM for 90 min at 4°C. Lysates were incubated with α-Flag or α-V5 conjugated dynabeads for 3 hr with constant rotation at 4°C [23]. For kinetochore purification, Dsn1-6His-3Flag strains were used. For the native yeast Dam1 complex purification, Dad1-3Flag or Dad1-3V5 was purified. For recombinant Dam1 complex, Spc34-Flag (used in Phosphorylation Kinase Assays below) was used and for yeast Cdk1, Cdc28-3V5 was used. Samples were washed three times with BH containing protease inhibitors, phosphatase inhibitors, 2 mM dithiothreitol (DTT) and either 150 mM KCl (for kinetochore purifications) or 400 mM KCl (for Dam1 complex purifications). Beads were further washed twice with BH containing 150 mM KCl and protease inhibitors. Associated proteins were eluted from the beads by gentle agitation of beads in elution buffer (0.5 mg/mL 3Flag peptide or 0.5 mg/ml 3V5 peptide in BH with 150 mM KCl and protease inhibitors) for 20-30 min at room temperature. Eluted samples were used or snap-frozen in liquid nitrogen and stored at −80°C.

Phosphatase treatment

Yeast lysates were incubated with Dynabeads conjugated with α-Flag or α-V5 antibodies to immobilize Dam1c and separate it from the cell lysate (described above in Protein biochemistry). Prior to elution from the beads, the Dam1c was incubated for 30 min with

lambda phosphatase at 30°C (BH 0.15, 1 mM MnCl2, 22 units-Lambda Protein Phosphatase; New England Biolabs, P0753L). Control samples contained phosphatase inhibitors. The Dam1c was then washed and eluted as described above.

Immunoblot and silver stain analysis

For immunoblot analysis, cell lysates were prepared as described above (Protein biochemistry section). Protein samples were separated using pre-cast 4%–12% or 10% Bis Tris Protein Gels (Thermo-Fisher) and standard procedures for sodium dodecyl sulfate-polyacrylamide gel electrophoresis (SDS-PAGE) and immunoblotting were followed as described in [23]. A 0.45 μm nitrocellulose membrane (BioRad) was used to transfer proteins from polyacrylamide gels. Commercial antibodies used for immunoblotting were: α-Flag, M2 (Sigma-Aldrich) 1:3,000; α-GFP, JL-8 (Living Colors) 1:5,000; α-Myc, 9E10 (Covance) 1:10,000; A polyclonal α-Dam1c antibody was generated by injecting recombinant Dam1c into rabbits at Pacific Immunology (Ramona, CA). The serum was then used 1:500. The secondary antibodies used were a sheep α-mouse antibody conjugated to horseradish peroxidase (HRP) (GE Life sciences) at a 1:10,000 dilution or a donkey α-rabbit antibody conjugated to HRP (GE Life sciences) at a 1:10,000 dilution. Antibodies were detected using the Super Signal West Dura Chemiluminescent Substrate (Thermo Scientific). For analysis by silver stain, the gels were stained with Silver Quest Staining Kit (Invitrogen).

In vitro binding assays

To examine the binding of Dam1c to Dad1-1 kinetochores, Dam1c was first fluorescently labeled. Dam1c (Dad1-SNAP-3V5) was purified as described above and then incubated in buffer containing SNAP-Surface 647 dye (10 μM in BH 0.15 M KCl and phosphatase and protease inhibitors) for 30 min with continuous gentile agitation while immobilized on beads. The excess dye was washed away with three washes of BH 0.15 M KCl and protease inhibitors and then the Dam1c was eluted. To test the interaction of Dam1c with kinetochores, the Dad1-1 kinetochores was also fluorescently labeled using CLIP-surface 547 dye and purified as described above and immobilized on α-Flag dynabeads. They were incubated with three-fold dilutions of purified Dam1c (starting at 9 ng) in buffer BH 0.15 M KCl and phosphatase and protease inhibitors for 30 min at room temperature with continuous gentile agitation. Beads were then washed three times with BH containing 150 mM KCl and protease inhibitors. Kinetochore bound to beads were eluted as described above.

Phosphorylation kinase assays

Yeast lysates were incubated with Dynabeads conjugated with α-V5 antibodies to isolate Cdk1 (Cdc28-3V5) from the cell lysate and it was subsequently eluted from beads (described above in Protein biochemistry). Soluble Cdk1 was then incubated for 30 min with soluble rDam1c (Spc34-Flag) in MOPS Assay Buffer (MAB) for 30 min at room temperature with continuous agitation (MAB, 25 mM MOPS, 15 mM MgCl2, 5 mM EGTA) containing protease inhibitors and phosphatase inhibitors with 0.8 mM ATP. Control samples excluded Cdk1. Samples were then incubated with Dynabeads conjugated with α-Flag antibodies to immobilize the rDam1c, which was then washed and eluted as described above and either analyzed by silver stain SDS-PAGE or added to the optical trap at 2 nM as described below.

Spotting assay and chromosome loss assay

For the spotting growth assay, the desired strains were grown overnight in YPD medium. The following day, cells were serially diluted 5-fold and spotted on YPD or YPD+ Benomyl (7.5 μg/mL). Plates were incubated at 23°C for 3 days or 37°C for 2 days. The chromosome loss assay techniques are described in [41]. Briefly, strains were grown on -URA plates to ensure selection for the chromosome fragment. The following day, the strains were diluted in water and spread onto YPD plates containing a fifth fold dilution of adenine (Adenine 0.001%). Cells were diluted to obtain about 200 colonies/plate and then grown at 23°C for 7-12 days before placing them at 4°C for 2-3 days. Total colonies and colonies with red sectoring were counted.

Analysis of kinetochore biorientation

Cells were arrested in metaphase by repressing *CDC20*, an activator of the anaphase promoter complex (APC), using the methionine promoter (*pMET3*) that is conditionally suppressed by methionine. Cells were first grown at room temperature in media lacking methionine to OD_{600} ~0.3 and then shifted to 37°C in the presence of CuSO4 (see below) and methionine to arrest cells in metaphase. Strains also carried an integrated tandem array of LacO sequences at centromere III and a *pCUP1-lacI-GFP* fusion that was induced by the addition of 0.25 mM CuSO4. Following 2.5 hours of incubation, cells were harvested and fixed with 3.7% formaldehyde in 100 mM phosphate buffer (pH 6.4) for 5-10 minutes. Cells were washed once with 100 mM phosphate (pH 6.4), resuspended in 100 mM phosphate, 1.2 M sorbitol buffer (pH 7.5) and permeabilized with 1% Triton X-100 containing 2 μg/ml DAPI (4', 6-diamidino-2-phenylindole; Molecular Probes). Cells were imaged using a Nikon E600 microscope with a 60X objective (NA = 1.40). Five Z stacks (0.3 micron apart) were acquired and all frames with nuclear signal in focus were maximally projected. NIS Elements software (Nikon) was used for image acquisition and processing [62].

Recombinant protein expression and purification

All ten *S. cerevisiae* Dam1 complex subunits were expressed in *E. coli* (BL21 Rosetta 2; Novagen, Madison, WI) from a single polycistronic vector [18]. The complex was affinity purified using a C-terminal 6xHis-tag or Flag-tag on Spc34p, and subjected to gel filtration, as previously described [15, 33, 51, 57]. For TIRF microscopy experiments, the Dam1 complex was tagged with a C-terminal

GFP tag on Dad1 protein. The *S. cerevisiae* Ndc80 complex was expressed in *E. coli*, using a C-terminal 6xHis-tag before being subjected to gel filtration, as previously reported [15, 51, 63, 64].

TIRF microscopy

Flow chambers were constructed using glass slides and functionalized coverslips as reported before [15, 33]. Coverslips were adhered to a glass slide with double-sided tape, to form individual flow channels between two adjacent strips of tape. 'Rigor' kinesin was added to each channel to nonspecifically bind to the coverslip. This allowed for the addition and immobilization of taxol-stabilized microtubules. 50 pM GFP-tagged Dam1c ^{Ask1} or Dam1c$^{Ask1\text{-}2D}$ was used to test the direct binding of the Dam1c to microtubules. For testing oligomerization on microtubules, an additional 1 nM of the untagged Dam1 complex was incubated. For testing the interaction between the Dam1 and Ndc80 complexes, 50 pM GFP-tagged Ndc80 complex was incubated alone or in the presence of 5 nM untagged Dam1c ^{Ask1} or Dam1c $^{Ask1\text{-}2D}$ to ensure Dam1 complex oligomerization. All TIRF assays were carried out in BRB80 (80 mM K-PIPES, 1 mM MgCl2, 1 mM EGTA, pH 6.9) in the presence of oxygen scavenger system (200 mg/ml glucose oxidase, 35 mg/ml catalase, 25mM glucose and 5mM dithiothreitol). Experiments using GFP-tagged Dam1 complex had an additional 0.8 mg/mL κ-casein and 50mM KCl. Experiments using GFP-tagged Ndc80 complex had an additional 8 mg/ml BSA.

Single particle tracking and analysis was carried out with custom software (available on request and developed in LabVIEW (National Instruments) and Igor Pro (Wavemetrics) [15, 19, 33, 65]. Mean residence times were carried out through bootstrapping analysis [19, 51]. Each residence time dataset was randomly resampled with replacement. All the datasets presented formed normal distributions; mean and standard deviation of the bootstrapped dataset are reported. The raw data is available in Data S1.

Optical trap assays

Optical trap-based bead motility assays were performed as in [23, 62]. Streptavidin-coated 0.56-μm polystyrene beads (Spherotech) were functionalized with biotinylated anti-penta-His antibody (QIAGEN) and stored in BRB80 containing 8 mg/ml BSA and 1 mM DTT at 4°C with continuous rotation. Beads were decorated with purified kinetochores (via Dsn1-6His-3Flag) in a total volume of 20 μL incubation buffer (BRB80 containing 1.5 mg/mL κ-casein). Kinetochore particles were diluted such that the concentration of Dsn1-6His-3Flag was ~0.4 ng/uL, and then incubated with 6 pM beads for 1 h at 4°C. For native Dam1c add back, kinetochores received a final concentration of ~2 nM. The concentration of rDam1c and nDam1c were obtained by comparing the intensity of Spc34 and Duo1 to dilutions of BSA standards on silver-stained SDS-PAGE using a standard curve. The BSA standards and its derived equation were run on the same gel for the calculated Dam1c concentrations. Kinetochores were incubated in the microtubule growth buffer (see below). Dynamic microtubule extensions were grown from coverslip-anchored GMPCPP-stabilized microtubule seeds in a microtubule growth buffer consisting of BRB80, 1 mM GTP, 250 μg/ml glucose oxidase, 25 mM glucose, 30 μg/mL catalase, 1 mM DTT, 1.4-1.5 mg/mL purified bovine brain tubulin and 1 mg/mL κ-casein. Assays were performed at 23°C. Rupture force experiments were performed as in [23, 62]. Briefly, an optical trap was used to apply a force of ~1-4 pN in the direction of microtubule assembly. Once beads were observed to track with microtubule growth for a distance of ~100-300 nm (to ensure end-on attachment), the applied force was increased at a constant rate of 0.25 pN/s until bead detachment. Records of bead position over time were generated and analyzed using custom software (Labview and Igor Pro, respectively) and used to determine the rupture force, which was marked as the maximum force sustained by the attachment during each event. All rupture force measurements are reported in Table S1 and all rupture force experiments were additionally analyzed using a log-rank test that is reported in Table S2.

QUANTIFICATION AND STATISTICAL ANALYSIS

Data was statistically analyzed using Graph Pad PRISM 7 and the error bars in all main figures and supplemental figures represent standard error mean of the mean (SEM) unless otherwise stated. N is the number of events or data points collected. p values for rupture force events were determined using a two-tailed unpaired t test and this was done for data in Figures 1, 2, and S2. p values for survival plots/curves were analyzed using log rank test and this was done for data in Figure S4. p values for quantitative chromosome transmission fidelity were determined using Student's t test and this was done for data in Figure 3. Error bars from standard deviation of two independent experiments is reported for the biorientation assay in Figure 3. p values for residence time was determined using a two-tailed unpaired t test this was done for data in Figures 4 and S2.